Original Article

Enhanced detection of skull-base bone invasion in nasopharyngeal carcinoma: the supplementary diagnostic value of ^{18}fluorine-sodium fluoride (^{18}F-NaF) positron emission tomography/computed tomography (PET/CT) combined with magnetic resonance imaging (MRI)

Meina Liang[#], Xufeng Guo[#], Chengmao Guo, Jingxing Xiao

Department of Nuclear Medicine (PET-CT Centre), Affiliated Hospital of Guangdong Medical University, Zhanjiang, China

Contributions: (I) Conception and design: J Xiao; (II) Administrative support: J Xiao, X Guo; (III) Provision of study materials or patients: X Guo, C Guo; (IV) Collection and assembly of data: J Xiao, C Guo; (V) Data analysis and interpretation: J Xiao; (VI) Manuscript writing: All authors; (VII) Final approval of manuscript: All authors.

[#]These authors contributed equally to this work.

Correspondence to: Jingxing Xiao, MD, PhD. Department of Nuclear Medicine (PET-CT Centre), Affiliated Hospital of Guangdong Medical University, No. 57 Renmin South Road, Xiashan District, Zhanjiang 524013, China. Email: 13824828797@163.com.

Background: Nasopharyngeal carcinoma (NPC) originates in the nasopharyngeal mucosa, the lateral wall of the nasopharynx. A significant challenge in NPC management is skull-base bone invasion (SBBI), which affects prognosis and treatment planning. Magnetic resonance imaging (MRI) is the primary diagnostic tool for SBBI in NPC patients; however, the detection of SBBI can be challenging due to skull-base complexity and overlapping MRI signals. ^{18}fluorine-sodium fluoride (^{18}F-NaF) positron emission tomography/computed tomography (PET/CT) is an emerging imaging technique that has shown promise in detecting osseous lesions. This cohort study aimed to assess the supplementary diagnostic value of ^{18}F-NaF PET/CT in detecting SBBI in NPC patients compared to that of MRI alone.

Methods: Imaging data were retrospectively collected from ^{18}F-NaF PET/CT and head-and-neck MRI examinations conducted within a 7-day period. The sensitivity, specificity, and accuracy of ^{18}F-NaF PET/CT, MRI, and the combination of both modalities in detecting SBBI were individually assessed. Both lesion- and patient-based analyses were employed for the comparison. Cochran's Q test was used to compare the accuracy of these methods, while the Bonferroni-corrected McNemar test was used for the pairwise comparisons. The data analysis was performed using the R software package, and a significance level of $P<0.05$ was considered statistically significant.

Results: A total of 164 patients were enrolled in the study. Using ^{18}F-NaF PET/CT, MRI, and the combined modality of ^{18}F-NaF PET/CT with MRI, 97, 84, and 94 cases of SBBI were diagnosed, respectively. At the patient level, the diagnostic efficacy (sensitivity, specificity, and accuracy) was as follows: ^{18}F-NaF PET/CT had 100% sensitivity, 93.1% specificity, and 97.0% accuracy; MRI had 90.2% sensitivity, 98.6% specificity, and 93.9% accuracy; and the combination of ^{18}F-NaF PET/CT and MRI had 100% sensitivity, 97.2% specificity, and 98.8% accuracy. The accuracy rate of ^{18}F-NaF PET/CT combined with MRI were significantly higher than that of MRI alone ($P=0.034$). A total of 284, 243, and 276 SBBI lesions were diagnosed using ^{18}F-NaF PET/CT, MRI, and ^{18}F-NaF PET/CT combined with MRI, respectively. The diagnostic efficacy (sensitivity, specificity, and accuracy) at the lesion level was as follows: ^{18}F-NaF PET/CT had 99.6% sensitivity, 75.9% specificity, and 95.4% accuracy; MRI had 88.2%

sensitivity, 93.1% specificity, and 89.1% accuracy; and the combination of ^{18}F-NaF PET/CT with MRI had 100% sensitivity, 91.4% specificity, and 98.5% accuracy. The combination of ^{18}F-NaF PET/CT with MRI significantly improved the accuracy rate compared to that of MRI alone, and the difference was statistically significant (P<0.001).

Conclusions: The combined use of ^{18}F-NaF PET/CT and MRI significantly enhanced the diagnosis of SBBI in NPC patients, and the combined method had improved diagnostic sensitivity and accuracy than MRI alone.

Keywords: Nasopharyngeal carcinoma (NPC); ^{18}F-sodium fluoride positron emission tomography-computed tomography (^{18}F-NaF PET/CT); magnetic resonance imaging (MRI); skull-base bone invasion (SBBI)

Submitted Feb 07, 2024. Accepted for publication Aug 08, 2024. Published online Sep 12, 2024.
doi: 10.21037/qims-24-265
View this article at: https://dx.doi.org/10.21037/qims-24-265

Introduction

Nasopharyngeal carcinoma (NPC) is a malignant tumor that arises from the epithelial cells lining the nasopharynx, a region that connects the nasal cavity with the upper throat. The incidence of NPC varies in different regions, and has a notably higher prevalence in East Asian and Southeast Asian countries (1,2). Due to its close proximity to the skull-base bones, NPC often invades the bones, and has been reported to have an incidence rate as high as 55.9% (3). When skull-base bone invasion (SBBI) occurs, the latest clinical staging of NPC classifies the disease as at least stage T3 (4,5).

The presence of SBBI in NPC has profound implications for radiation therapy planning, clinical staging, and prognosis (6,7). Our preliminary research revealed that, compared to conventional clinical diagnosis, ^{18}fluorine-sodium fluoride (^{18}F-NaF) positron emission tomography/computed tomography (PET/CT) altered the clinical tumor-node-metastasis (TNM) staging for 12.1% of NPC patients, as well as the delineation of radiation therapy target areas for 5.2% of these patients (8). Consequently, the precise identification of SBBI in NPC patients is of great significance, as it can significantly influence treatment outcomes and patient prognosis.

Contrast-enhanced head-and-neck magnetic resonance imaging (MRI) is the preferred imaging modality for diagnosing and staging NPC due to its high sensitivity and specificity. MRI is capable of detecting bone marrow lesions prior to apparent bone destruction; however, its efficacy in identifying cortical bone lesions is limited (2,9). In recent years, advancements in multi-modal imaging have shown the limitations of MRI in diagnosing SBBI in NPC (3,10,11). Various factors, including the presence of sinus air cells, anemia, and chronic bone inflammation, can interfere with accurate imaging and pose significant challenges in the MRI-based diagnosis of SBBI in NPC (3,10).

^{18}F-NaF, a radiotracer specifically tailored for bone imaging, offers a unique window into bone blood flow and metabolism, achieving a remarkable bone-to-background ratio in a brief time frame (12). ^{18}F-NaF PET/CT enables the simultaneous acquisition of both anatomical and metabolic images of the entire skeletal system, including SBBI in NPC. Our previous study demonstrated the remarkable sensitivity and specificity of ^{18}F-NaF PET/CT in the diagnosis of SBBI in NPC (13), and showed its superior diagnostic efficacy compared to MRI (3). Despite the promising results of ^{18}F-NaF PET/CT in the diagnosis of SBBI in NPC, limited research has been conducted on its combined use with MRI. Therefore, the present study aimed to investigate the diagnostic value of integrating ^{18}F-NaF PET/CT with MRI in the detection of SBBI in NPC, and to compare its effectiveness with the use of MRI alone. We present this article in accordance with the STARD reporting checklist (available at https://qims.amegroups.com/article/view/10.21037/qims-24-265/rc).

Methods

Patients

A retrospective review of ^{18}F-NaF PET/CT images of NPC patients was conducted from 1 June 2017 to 30 August 2021 at the PET/CT Center of the Affiliated Hospital of Guangdong Medical University. To be eligible for inclusion in this study, the patients had to meet the following inclusion criteria: (I) had histopathological confirmation

of NPC; (II) had undergone both ^{18}F-NaF PET/CT and head-and-neck MRI within a 7-day interval; and (III) had standardized treatment and clinical and imaging follow-up data available for at least 6 months, including CT, MRI, and ^{18}F-NaF PET/CT data.

A total of 164 patients were enrolled in the study. The age of the patients ranged from 21–71 years (mean age: 50.13 years). Of the patients, 124 were male and 40 were female. Patient staging was determined according to the 8th edition of the American Joint Committee on Cancer (AJCC) TNM staging system (4). The study was conducted in accordance with the Declaration of Helsinki (as revised in 2013). The study was approved by the Ethics Committee of the Affiliated Hospital of Guangdong Medical University (No. PJXJS2022-012). Written informed consent was obtained from all the patients.

^{18}F-NaF PET/CT protocols

^{18}F-NaF PET/CT imaging was conducted in accordance with the guidelines established by the European Association of Nuclear Medicine (14). During the procedure, the patient received an intravenous injection of approximately 200 MBq of ^{18}F-NaF. PET data were acquired using the GE Discovery Elite 690 PET/CT scanner (General Electric Medical Systems, Milwaukee, WI, USA) at a mean ± standard deviation (SD) time of 64±6 minutes post-injection. A low-dose helical CT transmission scan was performed, using the following parameters: pitch: 0.984; current: 120–230 mAs; voltage: 120 kV; field-of-view display: 50.0 cm, slice thickness: 3.75 mm; and reconstructed slice thickness: 1.25 mm. The static emission scan encompassed the entire body, and the acquisition time of the GE Discovery-690 PET/CT scanner was 2 minutes per bed position. The sinogram data from the CT scans were corrected for dead time, decay, and photon attenuation, and then reconstructed into a 128×128 matrix. Image reconstruction was accomplished using a fully three-dimensional (3D) maximum likelihood ordered subset expectation-maximization algorithm.

MRI protocols

A 3 Tesla MRI scanner equipped with a 32-channel head coil (MR750, General Electric, Chicago, USA) was used for the head-and-neck scan. Axial (parallel to the cranial base), sagittal, and coronal (parallel to the C3 vertebra) scans were performed. The scanning sequences included sagittal T1-weighted imaging (SAG-T1WI), axial T1-weighted imaging (AX-T1WI), axial T2-weighted imaging (AX-T2WI), coronal short tau inversion recovery (COR-STIR), axial T1-weighted imaging with contrast (AX-T1WIC+), coronal T1-weighted imaging with contrast (COR-T1WIC+), and sagittal T1-weighted imaging with contrast (SAG-T1WIC+).

Image interpretation

The PET/CT and MRI data sets were evaluated on dedicated workstations (GE Advantage workstation, version 4.6; GE Healthcare Life Sciences). All the images were thoroughly analyzed by two investigators, each of whom had successfully passed their respective board examinations in their specialized fields. Both were responsible for evaluating all the data sets. One investigator was a nuclear medicine physician with 5 years of experience in MRI, and the other investigator was a radiologist with 12 years of experience in PET/CT. The investigators interpreted the (I) ^{18}F-NaF PET/CT images, (II) MRI images, and (III) ^{18}F-NaF PET/CT images combined with MRI images. Any initial differences of opinion were resolved by consensus. The investigators were aware of the study protocol and the clinical information of patients but blinded to the results from the other imaging modalities. To reduce image reading interference, each imaging examination database was accessed after an interval of more than one month.

^{18}F-NaF PET/CT

PET component: a focal abnormal concentration of radioactivity in the skull-base bone, targeted as a malignant lesion Because of the heterogeneity of ^{18}F-NaF concentration in different bones, we could not establish a unified maximum standard unit value to evaluate all skeletons.

CT component: bone destruction or the osteoblastic manifestation of bone (local and asymmetric lesions with increased density) was targeted as the malignancy.

The final diagnosis was based on the overall findings from both the PET and CT components.

MRI: the diagnosis of SBBI was made using MRI, guided by the following criteria: (I) the presence of a defect in the low-signal intensity of the bone cortex on T1-weighted imaging (T1WI); and (II) the replacement of high-signal intensity marrow by low-signal intensity tissue on T1WI with an obvious enhancement observed in the enhanced scan (7,15,16). During the assessment process, the specific

Table 1 Basic data characteristics of 164 patients with NPC

Characteristics	Value (n=164)
Gender	
Male	124
Female	40
Age (years) (mean ± standard deviation)	50.13±11.95
Pathological typing	
Undifferentiated non-keratinizing carcinoma	160
Differentiated non-keratinizing carcinoma	4
T staging	
T1	4
T2	49
T3	74
T4	37

NPC, nasopharyngeal carcinoma.

locations and the extent of SBBI were recorded, ensuring a comprehensive and detailed analysis of the MRI data.

Combined ^{18}F-NaF PET/CT with MRI

If both ^{18}F-NaF PET/CT and MRI yielded positive results, a positive diagnosis indicating the presence of SBBI was established. Conversely, a negative diagnosis indicating the absence of SBBI was established when both modalities produced negative results. In cases in which a discrepancy arose between the two techniques, with one modality indicating a negative result and the other a positive result, the reviewing physicians exercised their judgement. This decision-making process was guided by multiple factors, including the combined characteristics of the two imaging techniques, lesion morphology, the degree of uptake/signal changes, and the relationship with adjacent tissues.

Reference standard

The final diagnosis of SBBI in the patients was established through a rigorous and comprehensive evaluation that integrated the imaging results with clinical follow-up results (median: 17 months; range, 6.5–28 months). Given the impracticality of obtaining biopsies from the SBBI lesions, the confirmation of SBBI presence relied heavily on pre-treatment contrast-enhanced MRI and subsequent follow-up imaging modalities, such as ^{18}F-NaF PET/CT, MRI, or CT. During the follow-up period, the diagnosis of SBBI was based on the following two key criteria: (I) a reduction in the volume of skull-base bone lesions following anti-cancer treatment, an increase in bone repair density on CT, or a decrease in enhancement intensity on MRI, and/or metabolic activity on PET, indicating positive lesions identified in earlier examinations; and (II) an increase in the size of the skull-base bone lesions and/or metabolic activity in the absence of anti-cancer treatment, indicating positive lesions. When met, these criteria served to confirm the presence of SBBI in the patients, thus establishing the final diagnosis.

Statistical analysis

The data analysis encompassed both patient- and lesion-level assessments. Diagnostic performance indicators were evaluated using dichotomous variables, encompassing the calculation of multiple metrics, including the positive-predictive value (PPV), negative-predictive value (NPV), sensitivity, specificity, and accuracy. Statistical comparisons among the different imaging modalities were conducted using Cochran's Q test. Pairwise comparisons were conducted using the McNemar test, incorporating the Bonferroni method for correction. The data analyses were performed using R software (version 3.4.3, accessible at http://www.r-project.org). A P value <0.05 was considered statistically significant.

Results

Patients' clinical characteristics

A total of 164 patients were included in the study, among whom, 92 (56.1%) developed SBBI. The most frequent site of SBBI was the clivus, accounting for 78.3% (72/92) of cases, followed by the greater wing of the sphenoid bone. *Tables 1* and *2* present a summary of the patients' clinical characteristics, and the location distribution of SBBI sites in NPC.

Diagnostic efficiency analysis in detecting SBBI in NPC

A total of 271 lesions of SBBI in NPC were identified in this study. The combination of ^{18}F-NaF PET/CT and MRI achieved a remarkable 100% detection rate for these lesions. When used individually, ^{18}F-NaF PET/CT detected

270 lesions, while MRI detected 239 lesions (*Table 3*). To assess the diagnostic capabilities of these imaging modalities, a patient-level analysis was conducted. The results revealed that ^{18}F-NaF PET/CT had excellent sensitivity (100%), specificity (93.1%), and accuracy (97.0%). MRI also performed admirably with a sensitivity of 90.2%, specificity of 98.6%, and accuracy of 93.9%. When combined, ^{18}F-NaF PET/CT and MRI achieved an impressive diagnostic performance with a sensitivity of 100%, specificity of 97.2%, and accuracy of 98.8% (*Table 4*). Further, the diagnostic performance was evaluated at the lesion level. ^{18}F-NaF PET/CT had high sensitivity (99.6%) and moderate specificity (75.9%), resulting in an accuracy of 95.4%. The MRI procedure had a sensitivity of 88.2%, specificity of 93.1%, and overall accuracy of 89.1%. Notably, the combined approach of ^{18}F-NaF PET/CT and MRI had a sensitivity of 100%, specificity of 91.4%, and accuracy of 98.5% (*Table 5*). In terms of statistical significance, the combined approach of ^{18}F-NaF PET/CT with MRI significantly outperformed MRI alone at the patient level (P=0.034). Similarly, at the lesion level, both ^{18}F-NaF PET/CT and the combined approach had significantly higher accuracy than MRI (both P<0.05). To provide a comprehensive overview, a detailed comparison of the diagnostic accuracy of the three modalities is presented in *Table 6*.

Table 2 The location distribution of the SBBI sites in NPC

SBBI (site)	Value (n=271)
Clivus	72
Great wing of sphenoid bone	62
Petrous apex of temporal bone	45
Inferior wall of the sphenoid sinus	38
Pterygoid process	39
Sphenoid bone	11
Occipital condyle	4

SBBI, skull-base bone invasion; NPC, nasopharyngeal carcinoma.

Discussion

NPC patients frequently experience SBBI; Li *et al.* reported

Table 3 Results of SBBI in NPC detection using ^{18}F-NaF PET/CT, MRI, and the combination of ^{18}F-NaF PET/CT with MRI

Examination techniques	Clivus	GWSB	APPOT	IWSS	Pterygoid process	Sphenoid bone	Occipital condyle	Total
PET/CT	72	62	44	38	39	11	4	270
MRI	70	49	43	36	31	6	4	239
PET/CT + MRI	72	62	45	38	39	11	4	271
Gold standard	72	62	45	38	39	11	4	271

SBBI, skull-base bone invasion; NPC, nasopharyngeal carcinoma; ^{18}F-NaF PET/CT, ^{18}F-sodium fluoride positron emission tomography-computed tomography; MRI, magnetic resonance imaging; GWSB, great wing of sphenoid bone; APPOT, apex partis petrosae ossis temporalis; IWSS, inferior wall of the sphenoid sinus.

Table 4 The diagnostic results at the patient-based level using ^{18}F-NaF PET/CT, MRI, and combined ^{18}F-NaF PET/CT with MRI (n=164)

Examination techniques	Negative by final diagnosis (n=72)		Positive by final diagnosis (n=92)		PPV (95% CI)	NPV (95% CI)	Sensitivity (95% CI)	Specificity (95% CI)	Accuracy (95% CI)
	Negative	Positive	Negative	Positive					
PET/CT	67	5	0	92	0.948 (0.902–0.989)	1.000 (1.000–1.000)	1.000 (1.000–1.000)	0.931 (0.875–0.986)	0.970 (0.945–0.994)
MRI	71	1	9	83	0.988 (0.964–1.000)	0.887 (0.824–0.947)	0.902 (0.837–0.957)	0.986 (0.958–1.000)	0.939 (0.902–0.97)
PET/CT + MRI	70	2	0	92	0.979 (0.948–1.000)	1.000 (1.000–1.000)	1.000 (1.000–1.000)	0.972 (0.931–1.000)	0.988 (0.97–1.000)

^{18}F-NaF PET/CT, ^{18}F-sodium fluoride positron emission tomography-computed tomography; MRI, magnetic resonance imaging; PPV, positive-predictive value; CI, confidence interval; NPV, negative-predictive value.

Table 5 The diagnostic results at the lesion-based level using ^{18}F-NaF PET/CT, MRI, and combined ^{18}F-NaF PET/CT with MRI (n=329)

Examination techniques	Negative by final diagnosis (n=58)		Positive by final diagnosis (n=271)		PPV (95% CI)	NPV (95% CI)	Sensitivity (95% CI)	Specificity (95% CI)	Accuracy (95% CI)
	Negative	Positive	Negative	Positive					
PET/CT	44	14	1	270	0.951 (0.931–0.971)	0.978 (0.925–1.000)	0.996 (0.989–1.000)	0.759 (0.638–0.862)	0.954 (0.933–0.973)
MRI	54	4	32	239	0.984 (0.968–0.996)	0.628 (0.553–0.713)	0.882 (0.845–0.919)	0.931 (0.862–0.983)	0.891 (0.854–0.924)
PET/CT + MRI	53	5	0	271	0.982 (0.964–0.996)	1.000 (1.000–1.000)	1.000 (1.000–1.000)	0.914 (0.845–0.983)	0.985 (0.970–0.997)

^{18}F-NaF PET/CT, ^{18}F-sodium fluoride positron emission tomography-computed tomography; MRI, magnetic resonance imaging; PPV, positive-predictive value; CI, confidence interval; NPV, negative-predictive value.

Table 6 The accuracy, sensitivity, and specificity comparison results for the three methods

Examination techniques	Accuracy		Sensitivity		Specificity	
	P_1	P_2	P_1	P_2	P_1[a]	P_2
PET/CT *vs.* MRI	0.342	0.001	0.001	0.001	–	0.012
PET/CT *vs.* PET/CT + MRI	1.000	0.259	1.000	1.000	–	0.028
MRI *vs.* PET/CT + MRI	0.034	<0.001	0.001	<0.001	–	0.001

P_1 represents the P value at the patient level; P_2 represents the P value at the lesion-based level; bonferroni adjustment was performed. [a], there was no difference in specificity based on the patient level. PET/CT, positron emission tomography-computed tomography; MRI, magnetic resonance imaging.

an incidence rate of up to 65.5% in a long-term follow-up study (16). In the present study, we identified 92 cases of SBBI in NPC, representing a prevalence of 56.1%. Notably, the clivus was the most frequently involved site, followed by the great wing of the sphenoid bone. These findings align with those reported in previous studies, highlighting the predilection of NPC for specific anatomical regions (3). The clivus is the most frequently invaded site in the skull base in NPC. This is likely due to its anatomical proximity to tumor-prone regions like the pharynx fossae and nasopharyngeal postero-superior wall. Tumor progression may lead to the invasion of adjacent tissues and extension through intracranial foramina, emphasizing the need for precise diagnosis and targeted treatment planning in NPC management (11).

With its exceptional spatial resolution, MRI is highly valuable in visualizing soft tissue and bone marrow, thus enabling the precise delineation of anatomical details and pathological changes (17). Consequently, MRI is the preferred imaging modality for evaluating SBBI in untreated NPC, particularly in the detection of bone marrow invasion, due to its superior spatial resolution and ability to visualize soft tissue and bone marrow details (18). However, the ability of MRI to accurately and comprehensively diagnose SBBI in NPC is limited (19). For instance, the sensitivity of MRI detection can be affected due to its susceptibility to interference from gas in the sinus wall of the skull base and its inability to clearly display the bone cortex. Additionally, chronic bone marrow inflammation and yellow marrow replacement can affect its diagnostic specificity. Previous studies have shown the superiority of ^{18}F-NaF PET/CT over MRI in identifying minor bone lesions, emphasizing its distinct advantage in SBBI detection (3). In addition to detecting SBBI, MRI is also employed to assess the extension of NPC into critical structures, including cranial nerves and intracranial regions. Therefore, MRI remains the primary imaging modality for NPC patients, particularly among newly diagnosed cases (20-23). The diagnostic potential of combining both imaging techniques for SBBI detection merits further exploration (13). To the best of our knowledge, this study is the first to investigate the value of combining ^{18}F-NaF PET/CT with MRI in the diagnosis of SBBI.

This study showed the remarkable sensitivity of ^{18}F-NaF PET/CT in detecting SBBI associated with NPC. Among the cohort of 92 (56.1%) patients with SBBI, MRI correctly identified SBBI in 84 (51.2%) patients, while ^{18}F-NaF PET/CT detected abnormal radioactive accumulation in 97 (59.1%) patients. Both imaging modalities detected SBBI in 83 (50.6%) patients (*Figure 1*). At the lesion level, ^{18}F-NaF PET/CT exhibited a high level of precision, identifying 270 (99.6%) of 271 lesions, surpassing the detection capabilities

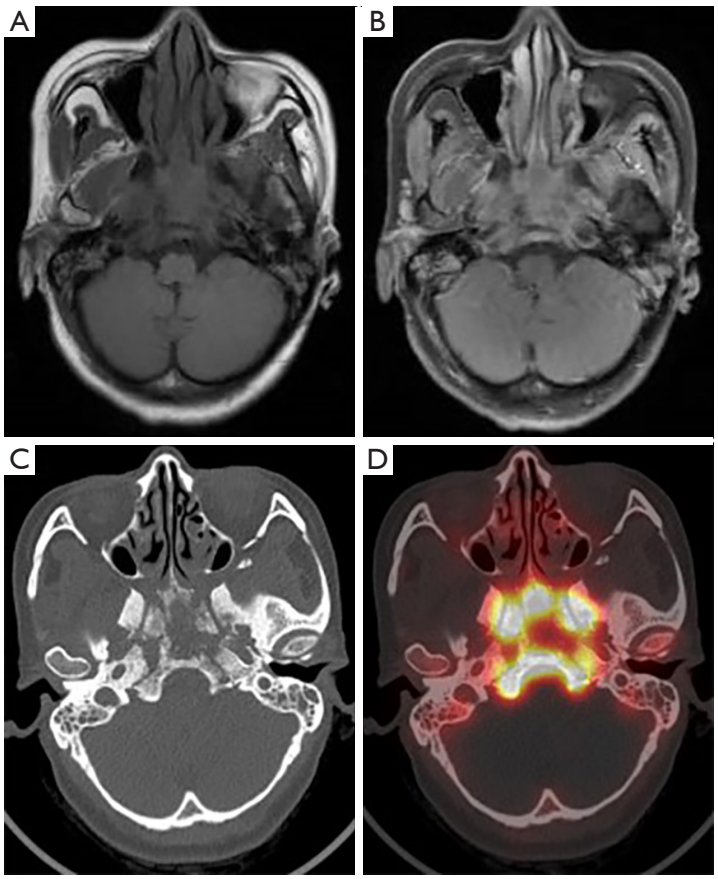

Figure 1 Images of a 45-year-old female patient diagnosed with NPC. (A) MRI-T1WI and (B) its contrast-enhanced variant demonstrated widespread SBBI, encompassing the clivus, sphenoid wing, and pterygoid process. (C) CT imaging revealed numerous osteolytic and osteogenic alterations in the skull-base bone. (D) The ^{18}F-NaF PET/CT image showed marked abnormal accumulation of ^{18}F-NaF in the lesions. The MRI observations were in agreement with the ^{18}F-NaF PET/CT findings in the detection of SBBI. NPC, nasopharyngeal carcinoma; MRI, magnetic resonance imaging; T1WI, T1-weighted imaging; CT, computed tomography; ^{18}F-NaF PET/CT, ^{18}F-sodium fluoride positron emission tomography-computed tomography; SBBI, skull-base bone invasion.

of MRI, which identified only 239 (88.2%) lesions. The ability of ^{18}F-NaF PET/CT to detect lesions compared to MRI was statistically significant (P=0.001), particularly lesions involving flat bones, such as the greater wing of the sphenoid and pterygoid process (*Figures 2,3*).

Zhang *et al.* (10) conducted a comparative study involving 52 patients with NPC, and used both ^{18}F-NaF PET/CT and MRI to detect SBBI. Their findings align with our own research findings; that is, they found that ^{18}F-NaF PET/CT successfully identified 178 SBBI lesions, while MRI only detected 135 lesions. There are several reasons for this discrepancy. First, the adult skull-base bone structure typically comprises a considerable amount of mature fat in the bone marrow, which appears as a uniformly high signal on T1WI. However, in clinical practice, various factors such as anemia (resulting in a mixture of red and yellow marrow) and magnetic susceptibility artifacts caused by air-containing tissues in the sphenoid sinus and nasopharynx can lead to uneven signal intensity in the skull-base bone on T1WI. Therefore, accurately using the abnormal signal of the skull base on MRI as a criterion for tumor invasion is challenging, primarily due to factors such as anemia and magnetic susceptibility artifacts (3). Conversely, as a bone-seeking radiotracer, ^{18}F-NaF predominantly reflects local bone blood flow and bone mineral exchange metabolism (24,25). enabling the earlier detection of bone lesions compared to morphological changes. Additionally, the detection of flat bones, such as the pterygoid process, poses

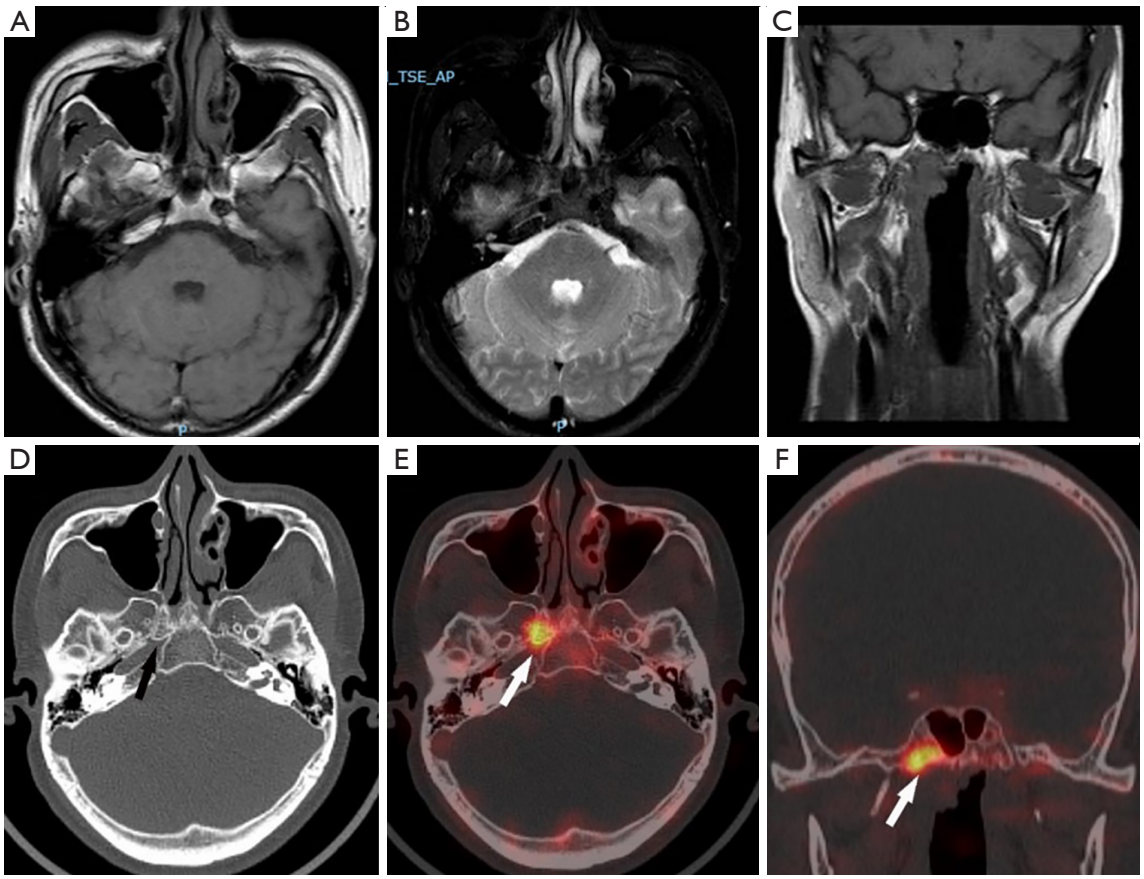

Figure 2 Images of a 29-year-old male patient with NPC. (A) MRI-T1WI, (B) T2WI, and (C) coronal T1WI exhibited no abnormal signals in the skull-base bone. (D) CT imaging (arrow) revealed no discernible bone destruction in the greater wing of the right sphenoid bone. However, (E,F) the ^{18}F-NaF PET/CT fusion images clearly delineated hypermetabolism at the corresponding site, as highlighted by the arrows, confirming the invasion of NPC. Hence, the integrated use of ^{18}F-NaF PET/CT with MRI was pivotal in diagnosing SBBI. NPC, nasopharyngeal carcinoma; MRI, magnetic resonance imaging; T1WI, T1-weighted imaging; T2WI, T2-weighted imaging; CT, computed tomography; ^{18}F-NaF PET/CT, ^{18}F-sodium fluoride positron emission tomography-computed tomography; SBBI, skull-base bone invasion.

challenges for MRI due to their limited bone marrow cavities and relatively thick cortical bone, which make it difficult to distinguish tumor invasion from normal bone invasion, especially when the tumor invades the cortical bone. Due to these advantages, ^{18}F-NaF PET/CT provides clearer images of small skull-base lesions than MRI. Thus, ^{18}F-NaF PET/CT is particularly suitable for depicting small bone lesions in the skull base. The integration of ^{18}F-NaF PET/CT with MRI holds the potential to enhance the identification of SBBI lesions. Our comparison of the sensitivity of combined ^{18}F-NaF PET/CT with MRI to that of MRI alone in the diagnosis of SBBI in NPC showed that the combined approach had significantly superior diagnostic capabilities ($P<0.05$).

In this study, 5 false-positive patients and 14 false-positive lesions were identified by ^{18}F-NaF PET/CT, exceeding the 1 false-positive patient and 4 false-positive lesions diagnosed by MRI. As a non-specific tumor imaging agent, ^{18}F-NaF tracer can lead to increased uptake and false positives in ^{18}F-NaF PET/CT imaging due to conditions such as inflammation of the adjacent sphenoid sinus wall and chronic inflammation of the bone marrow. Thus, a comprehensive analysis of ^{18}F-NaF PET/CT and MRI is recommended to effectively reduce false positives. Notably, the specificity of ^{18}F-NaF PET/CT combined with MRI was significantly higher than that achieved using a ^{18}F-NaF PET/CT diagnosis alone ($P<0.001$). This study showed that the integration of ^{18}F-NaF PET/CT with MRI significantly

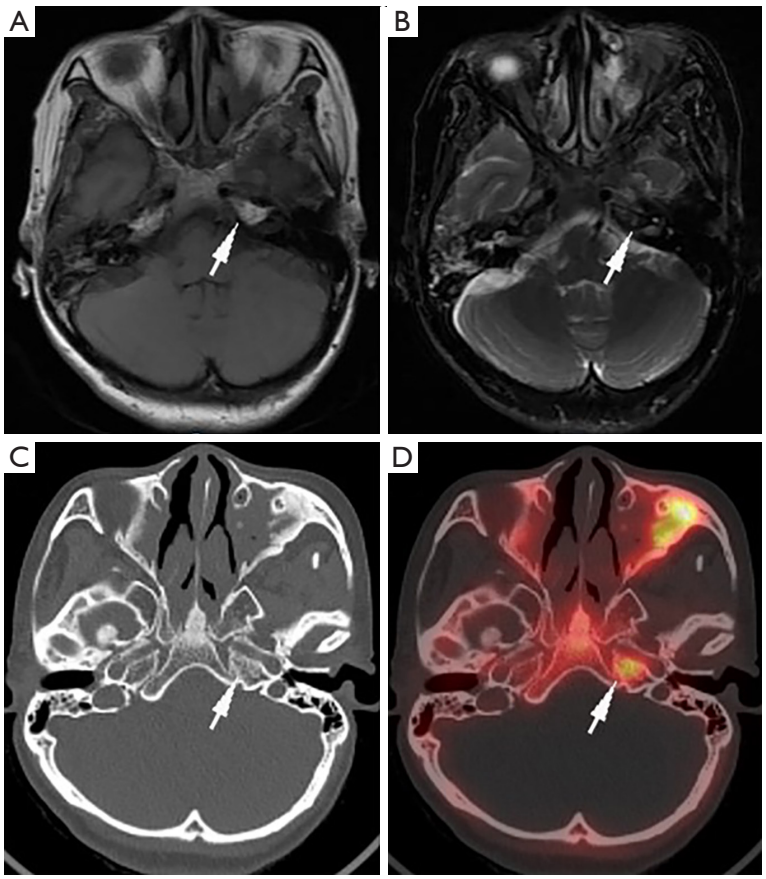

Figure 3 Images of a 41-year-old woman with NPC. (A) MRI-T1WI (arrow) and (B) T2WI (arrow) showed no abnormal signals in the left temporal bone. However, (C) CT revealed hyperdensity in the left temporal bone as indicated by the arrow, and (D) the ^{18}F-NaF PET/CT fusion image (arrow) subsequently demonstrated abnormal radioactive activity at the corresponding site, conclusively confirming tumor invasion in that region. This combined ^{18}F-NaF PET/CT and MRI approach effectively diagnosed SBBI. NPC, nasopharyngeal carcinoma; MRI, magnetic resonance imaging; T1WI, T1-weighted imaging; T2WI, T2-weighted imaging; CT, computed tomography; ^{18}F-NaF PET/CT, ^{18}F-sodium fluoride positron emission tomography-computed tomography; SBBI, skull-base bone invasion.

enhanced the diagnostic accuracy for SBBI in NPC patients compared to that of MRI alone ($P<0.05$). The primary advantage of this method lies in harnessing the superior sensitivity of ^{18}F-NaF PET/CT, enabling the detection of a broader range of skull-base lesions. Additionally, the comprehensive analysis of ^{18}F-NaF PET/CT in conjunction with multiple series of contrast-enhanced MRI images effectively mitigated the false-positive cases in the MRI diagnosis (*Figure 4*). Thus, the combined diagnosis using ^{18}F-NaF PET/CT and MRI had a superior level of accuracy than the MRI diagnosis alone.

In recent years, the use of PET/MRI in tumors of the head and neck has progressively increased. Research has shown that fluorodeoxyglucose (FDG)-PET/MR images exhibit superior discriminability than PET/CT images in mapping the tumor extension of sodium fluoride (NPC), particularly in cases of intracranial invasion (26,27). Further, the implementation of FDG and NaF dual-tracer imaging agents has proven feasible in clinical settings, exhibiting promising application value in initial clinical practice (28,29). Consequently, we posit that dual-tracer PET/MRI in NPC holds significant promise and merits further investigation.

However, it should be noted that this study had some limitations. First, the retrospective nature and limited sample size might have restricted the generalizability of the study's findings. Second, the reliance on clinical and imaging follow-ups for diagnostic criteria, due to the impracticality

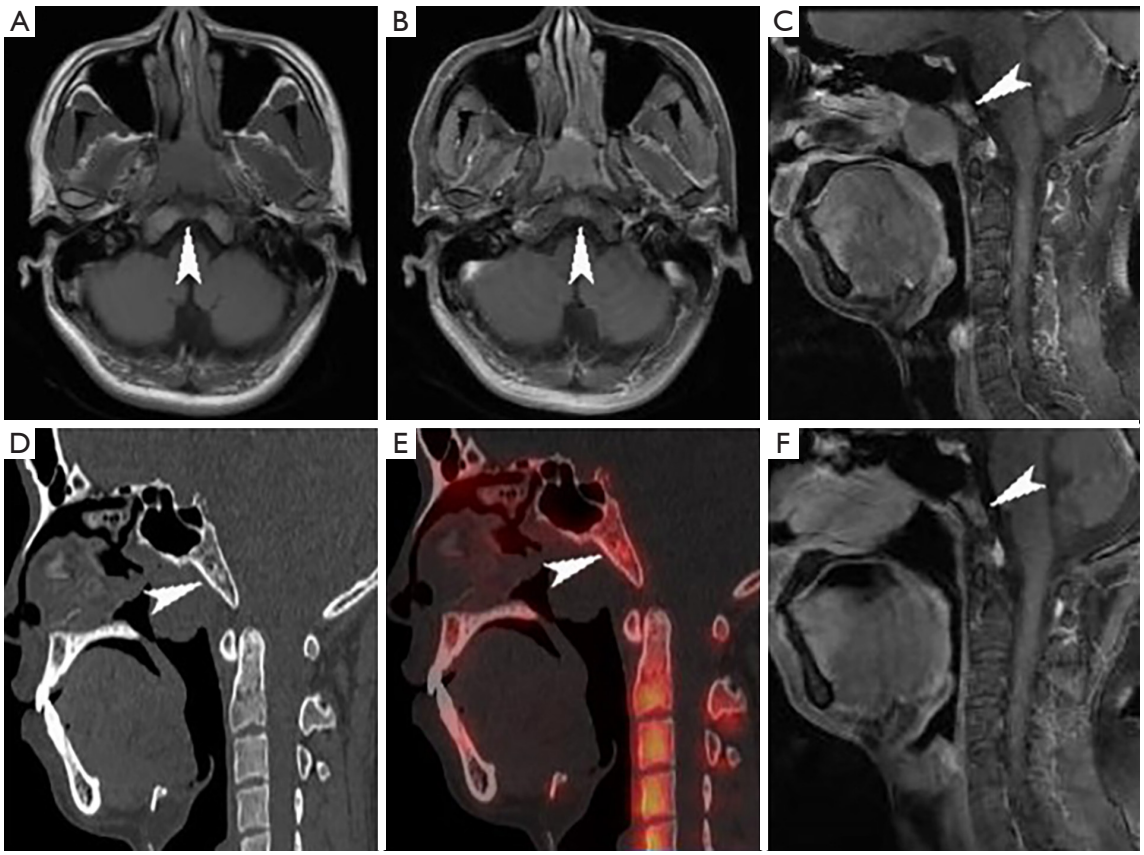

Figure 4 Images of a 29-year-old man with NPC. (A) MRI-T1WI images (arrowhead) revealed local hypointensity in the clivus. (B) Cross-sectional T1WI enhancement (arrowhead) and (C) sagittal T1WI enhancement (arrowhead) further indicated local enhancement, leading to a presumptive diagnosis of SBBI. (D) Sagittal CT (arrowhead) imaging demonstrated irregular increased density of the clivus. However, (E) the ^{18}F-NaF PET/CT fusion image (arrowhead) did not exhibit definite abnormal radiological activity at the corresponding site, suggesting a benign bone lesion when ^{18}F-NaF PET/CT was integrated with MRI findings. (F) A follow-up MRI 6 months later showed localized enhancement at the clivus (arrowhead), with no significant change compared to the initial MRI examination, ultimately confirming the diagnosis as a benign bone lesion. NPC, nasopharyngeal carcinoma; MRI, magnetic resonance imaging; T1WI, T1-weighted imaging; SBBI, skull-base bone invasion; CT, computed tomography; ^{18}F-NaF PET/CT, ^{18}F-sodium fluoride positron emission tomography-computed tomography.

of histopathological biopsies on skull-base lesions, might have introduced biases and subjectivity. Additionally, given the significant impact of SBBI on the T staging of NPC, and the fact that ^{18}F-NaF PET/CT can detect bone metastasis of NPC, further analysis is imperative to evaluate the influence of this imaging modality on staging and its potential to guide clinical treatment decisions.

Conclusions

The combined use of ^{18}F-NaF PET/CT and MRI significantly enhanced the diagnosis of SBBI in NPC patients, and the combined method had better diagnostic sensitivity and accuracy than MRI alone.

Acknowledgments

The authors would like to thank the patients and clinical staff involved in this study.

Funding: This study was funded by the Guangdong Basic and Applied Basic Research Fund (No. 2021A1515220052), the Zhanjiang Science and Technology Projects (No. 2021A05054), the Enhanced Research Initiation Program for Elite Scientists at the Affiliated Hospital of Guangdong Medical University

(No. GCC2023012), the 2024 Key Research Platforms and Projects of Ordinary Universities in Guangdong Province (No. 2024KTSCX163), and the Big Data Platform of Affiliated Hospital of Guangdong Medical University.

Footnote

Reporting Checklist: The authors have completed the STARD reporting checklist. Available at https://qims.amegroups.com/article/view/10.21037/qims-24-265/rc

Conflicts of Interest: All authors have completed the ICMJE uniform disclosure form (available at https://qims.amegroups.com/article/view/10.21037/qims-24-265/coif). The authors have no conflicts of interest to declare.

Ethical Statement: The authors are accountable for all aspects of the work in ensuring that questions related to the accuracy or integrity of any part of the work are appropriately investigated and resolved. The study was conducted in accordance with the Declaration of Helsinki (as revised in 2013). The study was approved by the Ethics Committee of the Affiliated Hospital of Guangdong Medical University (No. PJXJS2022-012). Written informed consent was obtained from all the patients.

References

1. Chen YP, Chan ATC, Le QT, Blanchard P, Sun Y, Ma J. Nasopharyngeal carcinoma. Lancet 2019;394:64-80.
2. Chen YP, Ismaila N, Chua MLK, Colevas AD, Haddad R, Huang SH, et al. Chemotherapy in Combination With Radiotherapy for Definitive-Intent Treatment of Stage II-IVA Nasopharyngeal Carcinoma: CSCO and ASCO Guideline. J Clin Oncol 2021;39:840-59.
3. Le Y, Chen Y, Zhou F, Liu G, Huang Z, Chen Y. Comparative diagnostic value of 18F-fluoride PET-CT versus MRI for skull-base bone invasion in nasopharyngeal carcinoma. Nucl Med Commun 2016;37:1062-8.
4. Pan XX, Tong LH, Chen YF, Li FL, Tang WB, Liu YJ, Yang W. A simplified T classification based on the 8th edition of the UICC/AJCC staging system for nasopharyngeal carcinoma. Cancer Manag Res 2019;11:3163-9.
5. He T, Yan RN, Chen HY, Zeng YY, Xiang ZZ, Liu F, Shao BF, Ma JC, Wang XR, Liu L. Comparing the 7th and 8th editions of UICC/AJCC staging system for nasopharyngeal carcinoma in the IMRT era. BMC Cancer 2021;21:327.
6. Gihbid A, Cherkaoui Salhi G, El Alami I, Belgadir H, Tawfiq N, Bendahou K, El Mzibri M, Cadi R, El Benna N, Guensi A, Khyatti M. Pretreatment [^{18}F]FDG PET/CT and MRI in the prognosis of nasopharyngeal carcinoma. Ann Nucl Med 2022;36:876-86.
7. Feng Y, Cao C, Hu Q, Chen X. Grading of MRI-detected skull-base invasion in nasopharyngeal carcinoma with skull-base invasion after intensity-modulated radiotherapy. Radiat Oncol 2019;14:10.
8. Wang D, Guo C, Xiao J. The potential advantages of (18)F sodium fluoride positron emission tomography-computed tomography for clinical staging and management planning in patients with nasopharyngeal carcinoma. Quant Imaging Med Surg 2024;14:3393-404.
9. Liao XB, Mao YP, Liu LZ, Tang LL, Sun Y, Wang Y, Lin AH, Cui CY, Li L, Ma J. How does magnetic resonance imaging influence staging according to AJCC staging system for nasopharyngeal carcinoma compared with computed tomography? Int J Radiat Oncol Biol Phys 2008;72:1368-77.
10. Zhang Y, Chen Y, Huang Z, Zhang L, Wan Q, Lei L. Comparison of (18)F-NaF PET/CT and (18)F-FDG PET/CT for Detection of Skull-Base Invasion and Osseous Metastases in Nasopharyngeal Carcinoma. Contrast Media Mol Imaging 2018;2018:8271313.
11. Zhang SX, Han PH, Zhang GQ, Wang RH, Ge YB, Ren ZG, Li JS, Fu WH. Comparison of SPECT/CT, MRI and CT in diagnosis of skull base bone invasion in nasopharyngeal carcinoma. Biomed Mater Eng 2014;24:1117-24.
12. Jadvar H. PET of Glucose Metabolism and Cellular Proliferation in Prostate Cancer. J Nucl Med 2016;57:25S-9S.
13. Xiao J, Wang D, Guo B, Wang L, Su M, Xu H. Observer agreement and accuracy of 18F-sodium fluoride PET/computed tomography in the diagnosis of skull-base bone invasion and osseous metastases in newly diagnosed

nasopharyngeal carcinoma. Nucl Med Commun 2020;41:942-9.
14. Beheshti M, Mottaghy FM, Paycha F, Behrendt FFF, Van den Wyngaert T, Fogelman I, Strobel K, Celli M, Fanti S, Giammarile F, Krause B, Langsteger W. (18)F-NaF PET/CT: EANM procedure guidelines for bone imaging. Eur J Nucl Med Mol Imaging 2015;42:1767-77.
15. Guo HH, Moradi F, Iagaru A. Clinical significance of extraskeletal computed tomography findings on 18F-NaF PET/CT performed for osseous metastatic disease evaluation. Nucl Med Commun 2016;37:975-82.
16. Li YZ, Cai PQ, Xie CM, Huang ZL, Zhang GY, Wu YP, Liu LZ, Lu CY, Zhong R, Wu PH. Nasopharyngeal cancer: impact of skull base invasion on patients prognosis and its potential implications on TNM staging. Eur J Radiol 2013;82:e107-11.
17. Gorolay VV, Niles NN, Huo YR, Ahmadi N, Hanneman K, Thompson E, Chan MV. MRI detection of suspected nasopharyngeal carcinoma: a systematic review and meta-analysis. Neuroradiology 2022;64:1471-81.
18. Lai V, Khong PL. Updates on MR imaging and ^{18}F-FDG PET/CT imaging in nasopharyngeal carcinoma. Oral Oncol 2014;50:539-48.
19. Zhan Y, Wang P, Wang Y, Wang Y, Tang Z. Dual-energy CT for the detection of skull base invasion in nasopharyngeal carcinoma: comparison of simulated single-energy CT and MRI. Insights Imaging 2023;14:95.
20. King AD, Woo JKS, Ai QY, Chan JSM, Lam WKJ, Tse IOL, Bhatia KS, Zee BCY, Hui EP, Ma BBY, Chiu RWK, van Hasselt AC, Chan ATC, Lo YMD, Chan KCA. Complementary roles of MRI and endoscopic examination in the early detection of nasopharyngeal carcinoma. Ann Oncol 2019;30:977-82.
21. Qi Y, Li J, Chen H, Guo Y, Yin Y, Gong G, Wang L. Computer-aided diagnosis and regional segmentation of nasopharyngeal carcinoma based on multi-modality medical images. Int J Comput Assist Radiol Surg 2021;16:871-82.
22. Yu E, O'Sullivan B, Kim J, Siu L, Bartlett E. Magnetic resonance imaging of nasopharyngeal carcinoma. Expert Rev Anticancer Ther 2010;10:365-75.
23. Glastonbury CM. Nasopharyngeal carcinoma: the role of magnetic resonance imaging in diagnosis, staging, treatment, and follow-up. Top Magn Reson Imaging 2007;18:225-35.
24. Dyrberg E, Larsen EL, Hendel HW, Thomsen HS. Diagnostic bone imaging in patients with prostate cancer: patient experience and acceptance of NaF-PET/CT, choline-PET/CT, whole-body MRI, and bone SPECT/CT. Acta Radiol 2018;59:1119-25.
25. Cui C, Li H, Ma H, Dong A, Xie F, Liang S, Li L, Zhou J, Xie C, Yan Y, Liu L. Staging of T2 and T3 nasopharyngeal carcinoma: Proposed modifications for improving the current AJCC staging system. Cancer Med 2020;9:7572-9.
26. Chan SC, Yeh CH, Yen TC, Ng SH, Chang JT, Lin CY, Yen-Ming T, Fan KH, Huang BS, Hsu CL, Chang KP, Wang HM, Liao CT. Clinical utility of simultaneous whole-body (18)F-FDG PET/MRI as a single-step imaging modality in the staging of primary nasopharyngeal carcinoma. Eur J Nucl Med Mol Imaging 2018;45:1297-308.
27. Cheng Y, Bai L, Shang J, Tang Y, Ling X, Guo B, Gong J, Wang L, Xu H. Preliminary clinical results for PET/MR compared with PET/CT in patients with nasopharyngeal carcinoma. Oncol Rep 2020;43:177-87.
28. Withofs N, Beguin Y, Cousin F, Tancredi T, Simoni P, Alvarez-Miezentseva V, De Prijck B, Hafraoui K, Bonnet C, Baron F, Hustinx R, Caers J. Dual-tracer PET/CT scan after injection of combined [^{18} F]NaF and [^{18} F]FDG outperforms MRI in the detection of myeloma lesions. Hematol Oncol 2019;37:193-201.
29. Christersson A, Larsson S, Sörensen J. Presurgical localization of infected avascular bone segments in chronic complicated posttraumatic osteomyelitis in the lower extremity using dual-tracer PET/CT. EJNMMI Res 2018;8:65.

Cite this article as: Liang M, Guo X, Guo C, Xiao J. Enhanced detection of skull-base bone invasion in nasopharyngeal carcinoma: the supplementary diagnostic value of ^{18}fluorine-sodium fluoride (^{18}F-NaF) positron emission tomography/computed tomography (PET/CT) combined with magnetic resonance imaging (MRI). Quant Imaging Med Surg 2024;14(10):7353-7364. doi: 10.21037/qims-24-265